Available online at www.sciencedirect.com
SCIENCE DIRECT®
Journal of Organometallic Chemistry 690 (2005) 1935–1946
Journal of Organometallic Chemistry
www.elsevier.com/locate/jorganchem

Synthesis and structural characterization of fluorenyltris(pyrazol-1-yl)borate ligands as new examples of cyclopentadienyl/scorpionate hybrid ligands

Susanne Bieller, Michael Bolte, Hans-Wolfram Lerner, Matthias Wagner *

Institut für Anorganische Chemie, J.W. Goethe-Universität Frankfurt, Marie-Curie-Strasse 11, D-60439 Frankfurt (Main), Germany

Received 4 November 2004; accepted 4 November 2004
Available online 11 February 2005

Abstract

Two fluorenyl/tris(pyrazol-1-yl)borate hybrid ligands, $FlBpz_3Li$ and $FlB(pz^{3\text{-}tBu})_3Li$, have been synthesized and structurally characterized by X-ray crystallography (Fl: 9-fluorenyl; pz: pyrazolyl). From the reaction of $FlBpz_3Li$ and $ZnCl_2$ in THF, the dinuclear complex $(THF)_3Lipz(Fl)Bpz_2ZnCl_2$ was obtained in which a $ZnCl_2$ moiety is chelated by two pyrazolyl ligands while the third pz ring coordinates to an $Li(THF)_3$ fragment. Acetonitrile solutions of the compound gradually transform into the mononuclear species $Fl(pz)Bpz_2Znpz_2B(pz)Fl$ featuring a distorted tetrahedral ZnN_4 core. In all molecular structures of $[FlBpz_3]^-$ or $[FlB(pz^{3\text{-}tBu})_3]^-$ complexes investigated so far, the hybrid ligands adopt very similar conformations with only two pyrazolyl rings bonded to the central metal, whereas the third pyrazolyl acts as dangling substituent. The fluorenyl substituent of $FlBpz_3Li$ may be deprotonated with KH in quantitative yield.

Keywords: Fluorenyl ligand; Scorpionate ligand; Zinc complex; X-ray crystallography

1. Introduction

Cyclopentadienyl derivatives [1,2] and tris(pyrazol-1-yl)borates (''scorpionates'') [3,4] are among the most popular ligands in transition metal chemistry. It therefore appeared interesting to us to combine both functionalities within the same molecule and thereby to create novel cyclopentadienyl/scorpionate hybrid ligands. Two coordination modes can be envisaged for these kinds of donor molecules: they may either adopt a bridging position between two different metal centres M^1 and M^2 (**A**, Fig. 1) or, alternatively, bind to the same metal atom M via the Cp ring and one or two of their pyrazolyl substituents (**B**, Fig. 1). Type **A** compounds **I**, **II** and **III** (Fig. 1) have already been synthesized and characterized by our group [5–10]. Only one example (**IV**, Fig. 1) of a type **B** transition metal complex is known in the literature up to now. Compound **IV** formed in a unique rearrangement reaction upon thermolysis of the corresponding complex $Sm[BH(pz^{3,5\text{-}Me})_3]_2(Cp)$ at 165 °C in the solid state [11]. **I**–**III** were prepared starting from ferrocene or cymantrene by treatment with BBr_3 [5–10]. This reaction, too, is of limited scope since only few other metal complexes exist (e.g. ruthenocene) which undergo electrophilic borylation without decay. It is therefore necessary to get access to derivatives of the free cyclopentadienyltris(pyrazol-1-yl)borate in order to be able to generate more sophisticated complexes **A** or **B**. As first example of a related class of ligands, the cyclopentadienyl/bis(pyrazol-1-yl)methane system [Li(bpzcp)(THF)] [bpzcp = 2,2-bis(3,5-dimethylpyrazol-1-yl)-1,

* Corresponding author. Tel.: +49 69 798 29156; fax: +49 69 798 29260.
E-mail address: Matthias.Wagner@chemie.uni-frankfurt.de (M. Wagner).

0022-328X/$ - see front matter © 2004 Elsevier B.V. All rights reserved.
doi:10.1016/j.jorganchem.2004.11.004

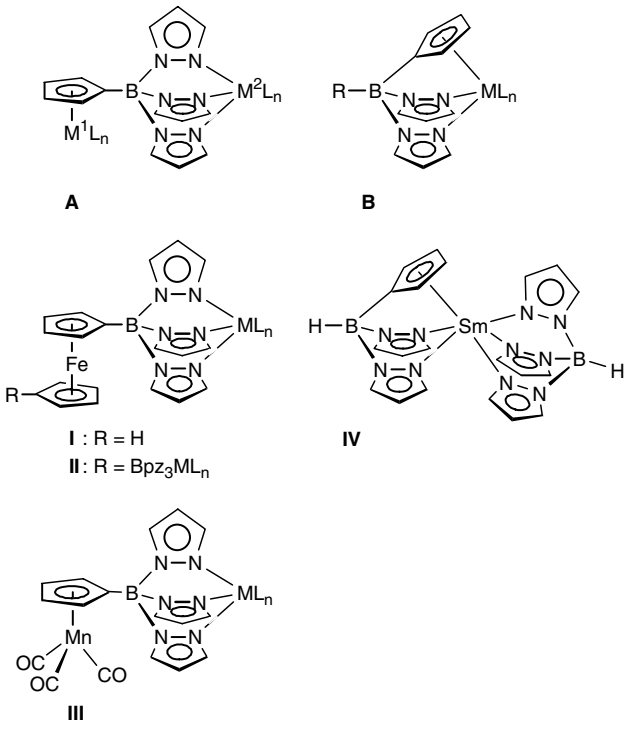

Fig. 1. Schematic representations of the bridging (**A**) and the chelating (**B**) coordination mode of cyclopentadienyl/tris(pyrazol-1-yl)borate hybrid ligands and of complexes **I**–**IV** for which these coordination modes have been realized. **IV**: CH_3 groups in the 3 and 5 positions of all pyrazolyl rings omitted for clarity.

1-diphenylethylcyclopentadienyl] was described by Otero, Fernández-Baeza and co-workers [12] early in 2004. Even more recently, Marques and co-workers [13] have published the tetramethylcyclopentadienyl functionalized scorpionate $[(C_5Me_4H)B(pz^{3\text{-}Me})_3]^-$ while our group has reported on the fluorenyl-based ligand $[FlBpz_3]^-$ [14] (Fl: 9-fluorenyl). In both cases, a similar synthesis protocol as the one developed for the transformation of ferrocenyl- and cymantrenylboranes into **I**–**III** was applied [5–10]. As far as the specific ligand design is concerned, we have chosen to use the fluorenyl rather than the cyclopentadienyl group mainly in order to avoid problems arising from Cp dimerisation.

The purpose of this paper is to describe the synthesis, structural characterization, and ligand behaviour of the fluorenylscorpionates $FlBpz_3Li$ and $FlBpz^{3\text{-}tBu}{}_3Li$. Moreover, we will present an optimized procedure for the deprotonation of the fluorenyl substituent in $FlBpz_3Li$.

2. Results and discussion

2.1. Syntheses and spectroscopy

Bis(dimethylamino)fluorenylborane (**1**) (Scheme 1) was employed as key starting material for all ligand syntheses described in this paper. The compound is conveniently accessible from fluorenyllithium and $BrB(NMe_2)_2$ in toluene. Reaction of **1** with 1 equivalent of Lipz ($Lipz^{3\text{-}tBu}$) and 2 equivalents of Hpz ($Hpz^{3\text{-}tBu}$) in refluxing toluene/THF for 8 h gives the fluorenylscorpionate ligand **2** (**3**) in excellent yield (pz: pyrazolide; Scheme 1). The zinc complex **4** is obtained upon treatment of **2** with $ZnCl_2$ in THF. An acetonitrile solution of **4** is not stable and gives crystals of **5** when stored at room temperature for several days (Scheme 1). Deprotonation of the fluorenyltris(pyrazol-1-yl)borate (**2**) is achieved quantitatively with KH as the base (**6**; Scheme 2). Attempts to use LiH, *n*-BuLi, *tert*-BuLi, $LiN(SiMe_3)_2$ or $Zn[N(SiMe_3)_2]_2$ instead either led to the formation of unwanted side products or even failed completely.

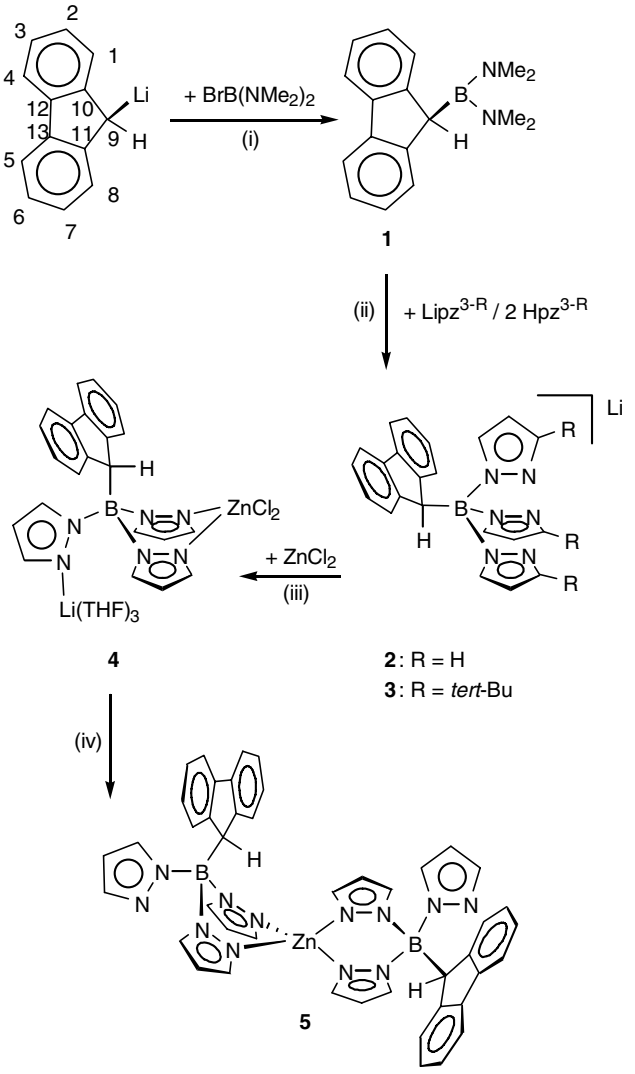

Scheme 1. Synthesis of compounds **1**–**5**. (i) Toluene, −78 °C to r.t.; (ii) toluene/THF, reflux temperature; (iii) **2**, THF, r.t.; (iv) CD_3CN, r.t.

The ^{11}B NMR spectrum of bis(dimethylamino)fluorenylborane (**1**) is characterized by a resonance at

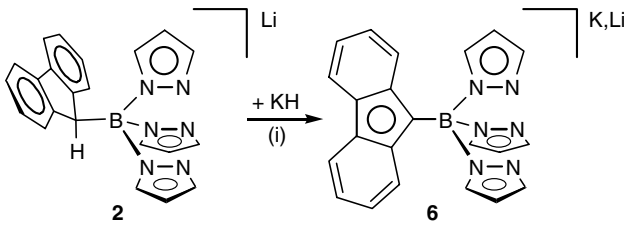

Scheme 2. Deprotonation of **2**. (i) THF, r.t.

$\delta(^{11}B) = 33.3$, typical of three-coordinate boron atoms bearing strongly π-donating substituents [15,16]. All other compounds **2**–**6** exhibit signals in the narrow range between $\delta(^{11}B) = 3.5$ and 1.7 which testify to the presence of four-coordinate boron nuclei. Two resonances are observed for the dimethylamino groups of **1** in the ^1H as well as in the ^{13}C NMR spectrum. This leads to the conclusion that rotation about the B–N bonds or the B–C bond is slow at room temperature on the NMR timescale. In the case of the parent fluorenyltris(pyrazol-1-yl)borate (**2**), one set of four well-resolved signals (two doublets and two virtual triplets; each signal integrates to 2H) is observed for the aromatic hydrogen atoms of the fluorenyl substituent, which points toward an unrestricted rotation about the boron–carbon bond; this conclusion is further supported by the signal pattern in the ^{13}C NMR spectrum. The aliphatic fluorenyl proton FlH-9 and the three pyrazolyl substituents of **2**, however, give rise to severely broadened resonances, which sharpen up considerably upon addition of potassium ions. We may therefore assume that the origin of the slow dynamic process responsible for line broadening lies in an Li–N association/dissociation equilibrium and that the lithium cation is not tightly bound to all three pyrazolyl rings at the same time in CD_3CN solution (cf. the molecular structure of **2**$(THF)_2$ in the solid state described below). At room temperature, the ^1H and ^{13}C NMR spectra of the *tert*-butyl substituted scorpionate **3** show the same general features as already discussed for the parent compound **2**, apart from the fact that the pyrazolyl signals of **3** are even broader. When the sample is cooled to 0 °C, two sets of proton resonances (intensity ratio 1:2), assignable to the pzH-4,5 atoms of two magnetically non-equivalent pyrazolyl rings, are detected. The signals of the unique pyrazolyl fragment are remarkably shifted to higher field strengths [$\delta(^1H) = 5.39$, 5.81].

Similar dynamic processes as in the case of **2** and **3** are observed in the ^1H and ^{13}C NMR spectra of the zinc complex **4**. At −20 °C, two magnetically equivalent pyrazolyl substituents and one unique pyrazolyl ring are detected. Thus, the scorpionate ligand most likely acts as a chelating four-electron donor to the zinc ion (cf. the X-ray crystal structure analysis of **4** and **5** below). On the basis of NMR spectroscopy, one cannot decide unequivocally whether each zinc atom binds one or two scorpionate ligands. (In the latter case, 0.5 equivalents of Zn^{2+} ions would have to be coordinated exclusively by chloride ions or CD_3CN solvent molecules since an equimolar ratio of scorpionate ligand and $ZnCl_2$ was employed in the synthesis of **4**.) There is, however, definitely only one species present in solution at −20 °C.

The most characteristic change that occurs to the ^1H NMR spectrum of **2** in THF upon addition of KH is the vanishing of the signal at $\delta(^1H) = 4.60$ which has to be assigned to the acidic fluorenyl proton FlH-9. Moreover, after deprotonation, the FlH-1,8 resonance is deshielded by 0.37 ppm [**2**: $\delta(^1H) = 5.41$, **6**: $\delta(^1H) = 5.78$], whereas FlH-2,7 [**2**: $\delta(^1H) = 6.82$, **6**: $\delta(^1H) = 6.45$] and FlH-3,6 [**2**: $\delta(^1H) = 7.11$, **6**: $\delta(^1H) = 6.35$] are more shielded by 0.37 and 0.76 ppm, respectively. All ^{13}C NMR signals of the fluorenyl substituent of **6** experience an upfield shift, which is most pronounced for FlC-3,6 [**2**: $\delta(^{13}C) = 125.2$, **6**: $\delta(^{13}C) = 109.7$; $\Delta\delta = -15.5$] and FlC-12,13 [**2**: $\delta(^{13}C) = 141.9$, **6**: $\delta(^{13}C) = 123.0$; $\Delta\delta = -18.9$]. NMR shift values of aromatic carbon atoms are particularly sensitive to changes in the π electron density [17]. Our NMR spectroscopic results thus point toward an increase of electronic charge within the fluorenyl π system which is in accord with the assumption that a partially delocalized electron lone pair has been generated by abstraction of FlH-9.

2.2. X-ray crystallography

The bis(dimethylamino)fluorenylborane (**1**) crystallizes from hexane in the trigonal space group $R\bar{3}$ (Table 1, Fig. 2). As to be expected, the boron atom adopts a planar configuration (sum of angles around boron: 360°) with only negligible deviations of the individual angles from the ideal value of 120°. The dihedral angle between the N(1)B(1)N(2) fragment and the best plane through the fluorenyl moiety was determined to be 71.3°.

In contrast to **1**, the lithium scorpionate **2**$(THF)_2$ (monoclinic, $P2_1/n$; from THF/hexane) features a four-coordinate boron centre with one fluorenyl and three pyrazol-1-yl substituents (Fig. 3). Both the boron–carbon bond and the boron-nitrogen bonds are substantially longer [B(1)–C(1) = 1.643(2) Å, B(1)–N(31) = 1.564(2) Å, B(1)–N(41) = 1.566(2) Å, B(1)–N(51) = 1.531(2) Å] than in **1** [B(1)–C(1) = 1.622(2) Å, B(1)–N(1) = 1.423(2) Å, B(1)–N(2) = 1.422(2) Å] which has to be attributed to the larger covalent radius of sp^3-hybridized as compared to sp^2-hybridized boron and to the lack of B–N π bonding in **2**$(THF)_2$. In addition to two THF ligands, each lithium cation of **2**$(THF)_2$ is bonded to two pyrazolyl rings whereas the third one merely acts as dangling side group with its free nitrogen atom pointing away from the fluorenyl substituent [C(1)–B(1)–N(51)–N(52) = 177.2(2)°]. The B–N bonds to the two lithium-coordinated pyrazolyl rings are longer by 0.033 Å [B(1)–N(31)] and 0.035 Å

Table 1
Crystal data and structure refinement details for compounds **1**, **2**$(THF)_2$, (**2**$DMSO)_2$, **2**$_2(THF)_2(DMSO)_2$, **3**THF, **4**, and **5**

Compound	**1**	**2**$(THF)_2$	(**2**$DMSO)_2$	**2**$_2(THF)_2(DMSO)_2$	**3**(THF)	**4**	**5**
Formula	$C_{17}H_{21}BN_2$	$C_{32}H_{38}BLiN_6O_{2.5}$	$C_{64}H_{80}B_2Li_2N_{12}O_6S_2$	$C_{56}H_{64}B_2Li_2N_{12}O_4S_2$	$C_{38}H_{50}BLiN_6O$	$C_{38}H_{50}BCl_2LiN_6O_4Zn$	$C_{48}H_{44}B_2N_{14}Zn$
Formula weight	264.17	564.43	1213.02	1068.81	624.59	808.86	903.96
Colour, shape	Colourless, block	Colourless, block	Colourless, plate	Colourless, needle	Colourless, block	Colourless, needle	Colourless, block
Crystal size (mm)	$0.42 \times 0.33 \times 0.29$	$0.47 \times 0.42 \times 0.36$	$0.21 \times 0.17 \times 0.11$	$0.21 \times 0.08 \times 0.07$	$0.42 \times 0.40 \times 0.19$	$0.47 \times 0.21 \times 0.18$	$0.19 \times 0.12 \times 0.08$
T (K)	100(2)	173(2)	100(2)	100(2)	100(2)	100(2)	100(2)
λ (Mo Kα radiation) (Å)	0.71073	0.71073	0.71073	0.71073	0.71073	0.71073	0.71073
Crystal system	Trigonal	Monoclinic	Triclinic	Orthorhombic	Monoclinic	Orthorhombic	Orthorhombic
Space group	$R\bar{3}$	$P2_1/n$	$P\bar{1}$	$Pbca$	$P2_1/c$	$P2_12_12_1$	$Pccn$
a (Å)	20.4154(19)	9.9397(7)	9.2733(15)	14.847(3)	22.492(3)	15.9419(8)	16.893(3)
b (Å)	20.4154(19)	18.8924(12)	11.850(2)	25.093(7)	15.8683(14)	16.9869(9)	15.740(3)
c (Å)	18.4574(17)	16.2666(13)	17.415(3)	30.713(8)	21.016(3)	29.4528(15)	16.235(3)
α (°)	90	90	106.059(13)	90	90	90	90
β (°)	90	92.317(6)	96.680(12)	90	104.077(11)	90	90
γ (°)	120	90	105.324(13)	90	90	90	90
V (Å^3)	6662.2(11)	3052.1(4)	1736.2(5)	11442(5)	7275.6(16)	7975.9(7)	4316.8(14)
Z	18	4	1	8	8	8	4
D_{calc} (g cm^{-3})	1.185	1.228	1.160	1.241	1.140	1.347	1.391
μ (mm^{-1})	0.069	0.079	0.132	0.149	0.069	0.796	0.623
Number of reflections collected	18757	36866	8801	27306	31617	50788	17084
Number of independent reflections	2808	6362	5989	11164	12157	15813	4192
R_{int}	0.0646	0.0588	0.0558	0.1977	0.0884	0.0605	0.3000
Data/restraints/parameters	2808/0/185	6362/0/388	5989/0/397	11164/0/703	12157/0/847	15813/0/955	4192/0/295
Goodness-of-fit	0.856	1.060	0.936	0.748	0.561	0.829	0.736
R_1, wR_2 ($I>2\sigma(I)$)	0.0361, 0.0667	0.0555, 0.1516	0.0886, 0.2299	0.1041, 0.2013	0.0414, 0.0706	0.0381, 0.0668	0.0726, 0.1253
R_1, wR_2 (all data)	0.0678, 0.0728	0.0724, 0.1617	0.1298, 0.2525	0.3693, 0.3236	0.1471, 0.0842	0.0594, 0.0700	0.2194, 0.1743
Largest difference peak and hole (e Å^{-3})	0.169 and −0.160	0.564 and −0.578	0.934 and −0.406	0.341 and −0.360	0.143 and −0.226	1.175 and −0.499	0.581 and −0.432

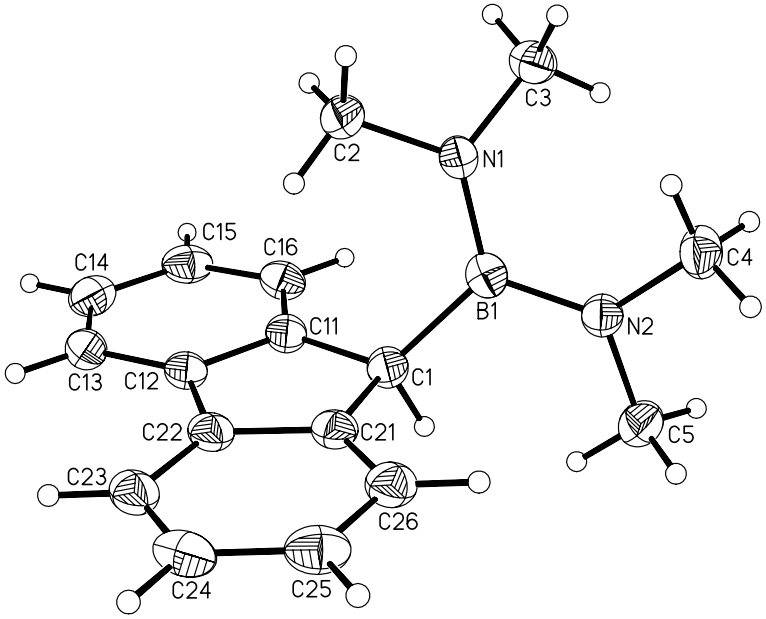

Fig. 2. Molecular structure and numbering scheme of compound **1**. Thermal ellipsoids are shown at the 50% probability level. Selected bond lengths (Å), angles (°), torsion angles (°), and dihedral angles (°): B(1)–C(1) = 1.622(2), B(1)–N(1) = 1.423(2), B(1)–N(2) = 1.422(2); N(1)–B(1)–N(2) = 121.5(1), N(1)–B(1)–C(1) = 120.3(1), N(2)–B(1)–C(1) = 118.2(1); C(1)–B(1)–N(1)–C(2) = 21.8(2), C(1)–B(1)–N(2)–C(5) = 18.1(2), N(1)–B(1)–C(1)–C(11) = 30.7(2), N(2)–B(1)–C(1)–C(11) = −151.2(1); N(1)B(1)N(2)//fluorenyl = 71.3.

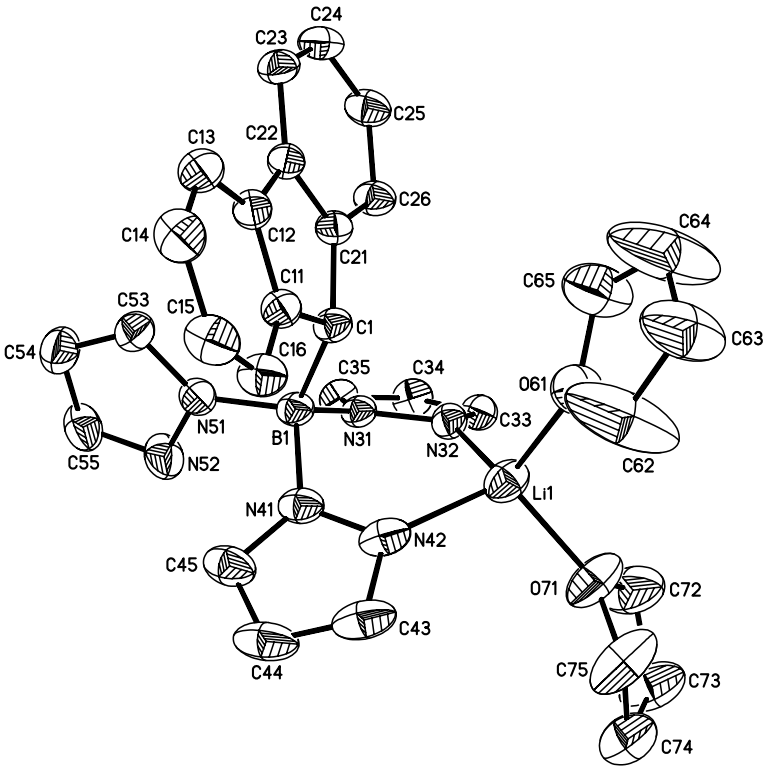

Fig. 3. Molecular structure and numbering scheme of compound **2**$(THF)_2$. Hydrogen atoms are omitted for clarity. Thermal ellipsoids are shown at the 50% probability level. Selected bond lengths (Å), angles (°), torsion angles (°), and dihedral angles (°): B(1)–C(1) = 1.643(2), B(1)–N(31) = 1.564(2), B(1)–N(41) = 1.566(2), B(1)–N(51) = 1.531(2), Li(1)–N(32) = 2.027(3), Li(1)–N(42) = 2.040(4), Li(1)–O(61) = 1.942(4), Li(1)–O(71) = 1.942(3); C(1)–B(1)–N(31) = 108.1(1), C(1)–B(1)–N(41) = 108.7(1), C(1)–B(1)–N(51) = 114.8(1), N(31)–B(1)–N(41) = 109.3(1), N(31)–B(1)–N(51) = 107.8(1), N(41)–B(1)–N(51) = 108.1(1), N(32)–Li(1)–N(42) = 97.5(2); C(1)–B(1)–N(31)–N(32) = 55.1(2), C(1)–B(1)–N(41)–N(42) = −55.2(2), C(1)–B(1)–N(51)–N(52) = 177.2(2); N(31)N(32)C(33)C(34)C(35)//N(41)N(42)C(43)C(44)C(45) = 49.4.

[B(1)–N(41)] than the boron-nitrogen bond to the uncomplexed pyrazolyl ring [B(1)–N(51) = 1.531(2) Å]. Structurally characterized lithium scorpionates are rare. The only examples listed in the current version of the Cambridge Structural Database [18] are the *tert*-butyl substituted tris(pyrazol-1-yl)borate $PhB(pz^{3\text{-}tBu})_3Li$ [19] and the ferrocene-based derivative $FcBpz_3Li$ [8]. In the case of $PhB(pz^{3\text{-}tBu})_3Li$, the lithium ion interacts with all three pyrazolyl rings of the scorpionate moiety. Further access of other ligands is prevented by steric hindrance. The compound therefore exists as a discrete mononuclear species with an uncommon trigonal coordination environment. The resulting Li–N bond lengths of 1.934(3), 1.977(3), and 1.979(3) Å are significantly shorter than the lithium-nitrogen bonds in **2**$(THF)_2$ with its distorted tetrahedral ligand sphere [Li(1)–N(32) = 2.027(3) Å, Li(1)–N(42) = 2.040(4) Å]. Very similar values are observed for the N–Li–N bond angle in **2**$(THF)_2$ [N(32)–Li(1)–N(42) = 97.5(2)°] and the corresponding angles in $PhB(pz^{3\text{-}tBu})_3Li$ [96.1(2)°, 97.6(2)°, 98.1(2)°]. $FcBpz_3Li$ forms centrosymmetric dimers in the solid state, in which each lithium ion binds to two tris(pyrazol-1-yl)borate ligands. Two pyrazolyl rings of each scorpionate fragment coordinate only one lithium ion, whereas the third pz substituent bridges two Li^+ centres.

Two kinds of single crystals were obtained upon layering a THF solution of **2**, to which a small amount of DMSO had been added, with toluene. The first sample [(**2**DMSO)$_2$; triclinic, $P\bar{1}$] consists of centrosymmetric dinuclear complexes in which two DMSO molecules act as bridging ligands between the lithium ions (Fig. 4). The dihedral angles between the planes of the non-coordinating pyrazolyl rings and the Li(1)O(1)-Li(1$^{\#}$)O(1$^{\#}$) core are 3.5°. The two fluorenyl substituents adopt an *anti* position with respect to the $Bpz_2Li\cdots Li^{\#}pz_2^{\#}B^{\#}$ backbone thereby preventing unfavourable steric interactions with the DMSO-methyl groups. In the second sample [**2**$_2$(THF)$_2$(DMSO)$_2$; orthorhombic, *Pbca*], two ligands $[FlBpz_3]^-$ coordinate one lithium ion in a chelating manner (Fig. 5). The second lithium ion is ligated by the oxygen atoms of two THF and two DMSO molecules. Thus, a distorted tetrahedral coordination environment is provided for all lithium ions both in (**2**DMSO)$_2$ and in **2**$_2$(THF)$_2$(DMSO)$_2$; the overall molecular structure and conformation of the scorpionate moiety is the same for all three species **2**$(THF)_2$, (**2**DMSO)$_2$ and **2**$_2$(THF)$_2$(DMSO)$_2$.

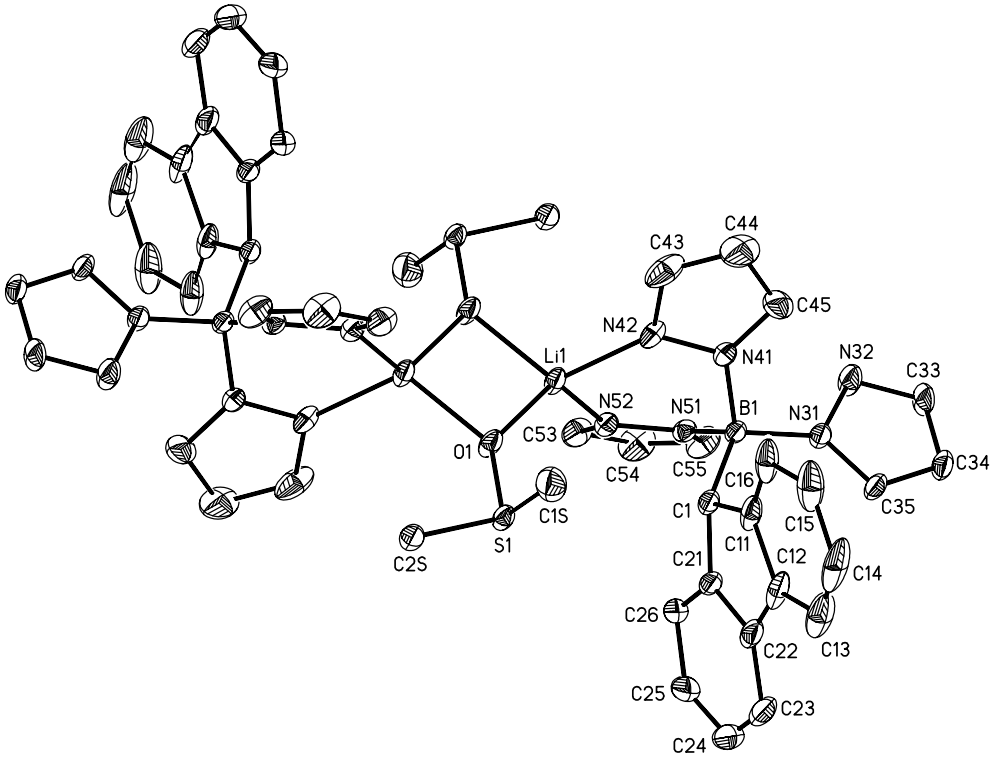

Fig. 4. Molecular structure and numbering scheme of compound (**2**DMSO)$_2$. Hydrogen atoms are omitted for clarity. Thermal ellipsoids are shown at the 50% probability level. Selected bond lengths (Å), angles (°), torsion angles (°), and dihedral angles (°): B(1)–C(1) = 1.635(6), B(1)–N(31) = 1.541(5), B(1)–N(41) = 1.573(5), B(1)–N(51) = 1.549(6), Li(1)–N(42) = 2.022(8), Li(1)–N(52) = 2.028(7), Li(1)–O(1) = 1.934(7), Li(1)–O(1$^{\#}$) = 1.953(7); C(1)–B(1)–N(31) = 114.6(3), C(1)–B(1)–N(41) = 108.2(3), C(1)–B(1)–N(51) = 109.6(3), N(31)–B(1)–N(41) = 107.3(3), N(31)–B(1)–N(51) = 107.9(3), N(41)–B(1)–N(51) = 109.2(3), N(42)–Li(1)–N(52) = 94.4(3); C(1)–B(1)–N(31)–N(32) = 179.9(4), C(1)–B(1)–N(41)–N(42) = −59.3(5), C(1)–B(1)–N(51)–N(52) = 57.2(4); N(41)N(42)C(43)C(44)C(45)//N(51)N(52)C(53)C(54)C(55) = 48.5, N(31)N(32)C(33)C(34) C(35)//Li(1)O(1)Li(1$^{\#}$)O(1$^{\#}$) = 3.5. Symmetry transformation used to generate equivalent atoms: $-x+1$, $-y+1$, $-z+1$ (#).

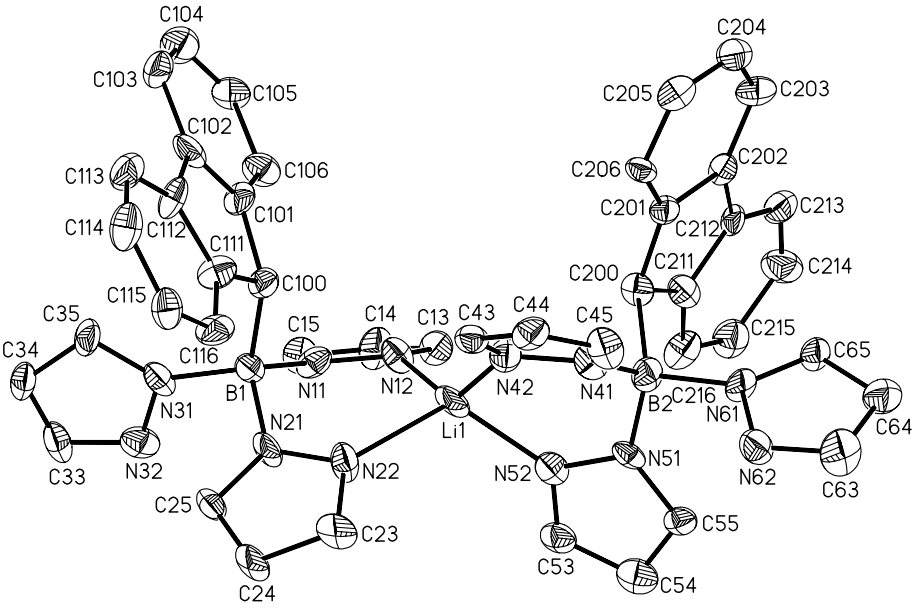

Fig. 5. Molecular structure and numbering scheme of compound $\mathbf{2}_2(THF)_2(DMSO)_2$. Hydrogen atoms and the $[Li(DMSO)_2(THF)_2]^+$ cation are omitted for clarity. Thermal ellipsoids are shown at the 50% probability level. Selected bond lengths (Å), angles (°), torsion angles (°), and dihedral angles (°): B(1)–C(100) = 1.62(2), B(2)–C(200) = 1.67(2), B(1)–N(11) = 1.62(2), B(1)–N(21) = 1.55(2), B(1)–N(31) = 1.57(2), B(2)–N(41) = 1.55(2), B(2)–N(51) = 1.50(2), B(2)–N(61) = 1.60(1), Li(1)–N(12) = 2.06(2), Li(1)–N(22) = 2.07(2), Li(1)–N(42) = 1.94(3), Li(1)–N(52) = 2.04(3); C(100)–B(1)–N(11) = 106(1), C(100)–B(1)–N(21) = 114(1), C(100)–B(1)–N(31) = 115(1), N(11)–B(1)–N(21) = 109(1), N(11)–B(1)–N(31) = 107(1), N(21)–B(1)–N(31) = 106(1), C(200)–B(2)–N(41) = 108(1), C(200)–B(2)–N(51) = 114(1), C(200)–B(2)–N(61) = 112(1), N(41)–B(2)–N(51) = 113(1), N(41)–B(2)–N(61) = 106(1), N(51)–B(2)–N(61) = 105(1), N(12)–Li(1)–N(22) = 94(1), N(12)–Li(1)–N(42) = 137(1), N(12)–Li(1)–N(52) = 104(1), N(22)–Li(1)–N(42) = 107(1), N(22)–Li(1)–N(52) = 120(1), N(42)–Li(1)–N(52) = 98(1); C(100)–B(1)–N(11)–N(12) = 59(1), C(100)–B(1)–N(21)–N(22) = –57(1), C(100)–B(1)–N(31)–N(32) = 173(1), C(200)–B(2)–N(41)–N(42) = 64(1), C(200)–B(2)–N(51)–N(52) = −59(1), C(200)–B(2)–N(61)–N(62) = 172(1); N(11)N(12)C(13)C(14)C(15)//N(21)N(22)C(23)C(24)C(25) = 48.7, N(41)N(42)C(43)C(44)C(45)//N(51)N(52)C(53)C(54)C(55) = 47.7.

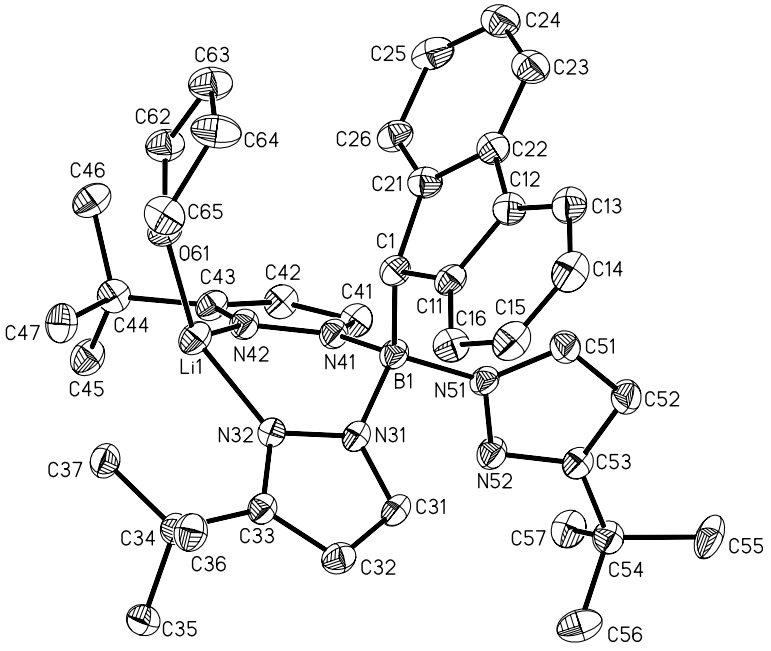

Fig. 6. Molecular structure and numbering scheme of compound **3**THF. Hydrogen atoms are omitted for clarity. Thermal ellipsoids are shown at the 50% probability level. Selected bond lengths (Å), angles (°), torsion angles (°), and dihedral angles (°): B(1)–C(1) = 1.632(5), B(1)–N(31) = 1.573(4), B(1)–N(41) = 1.566(5), B(1)–N(51) = 1.529(4), Li(1)–N(32) = 1.929(7), Li(1)–N(42) = 1.985(6), Li(1)–O(61) = 1.918(6); C(1)–B(1)–N(31) = 108.4(3), C(1)–B(1)–N(41) = 110.2(3), C(1)–B(1)–N(51) = 114.7(3), N(31)–B(1)–N(41) = 108.8(2), N(31)–B(1)–N(51) = 106.8(3), N(41)–B(1)–N(51) = 107.7(3), N(32)–Li(1)–N(42) = 96.7(3), N(32)–Li(1)–O(61) = 130.0(3), N(42)–Li(1)–O(61) = 115.6(3); C(1)–B(1)–N(31)–N(32) = 60.0(4), C(1)–B(1)–N(41)–N(42) = −66.5(3), C(1)–B(1)–N(51)–N(52) = 176.7(3); N(31)N(32)C(33)C(32)C(31)//N(41)N(42)C(43)C(42)C(41) = 50.3.

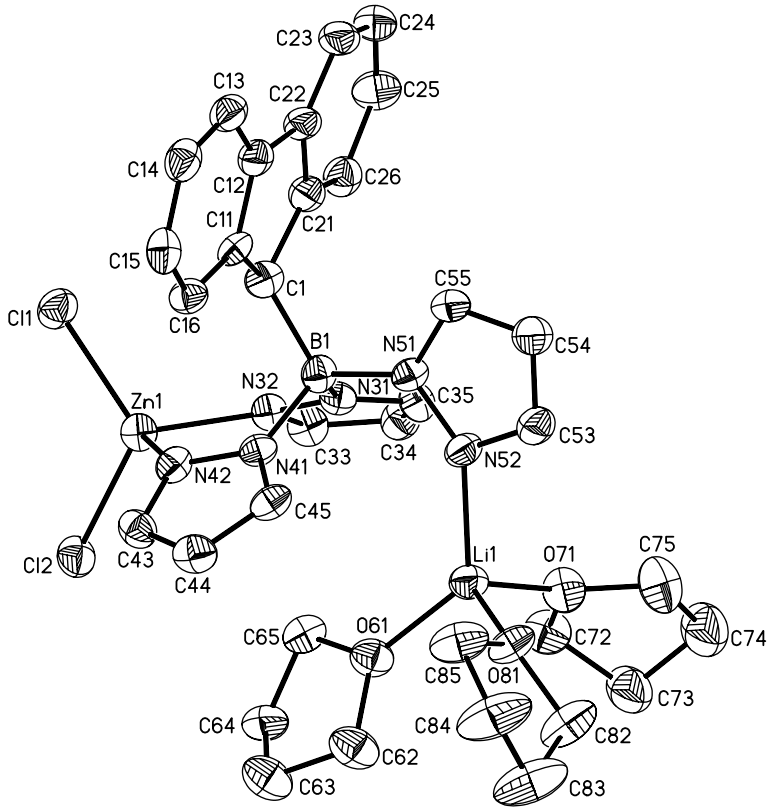

Fig. 7. Molecular structure and numbering scheme of compound **4**. Hydrogen atoms are omitted for clarity. Thermal ellipsoids are shown at the 50% probability level. Selected bond lengths (Å), angles (°), torsion angles (°), and dihedral angles (°): B(1)–C(1) = 1.626(5), B(1)–N(31) = 1.581(5), B(1)–N(41) = 1.562(5), B(1)–N(51) = 1.532(5), Zn(1)–N(32) = 2.045(3), Zn(1)–N(42) = 2.038(3), Li(1)–N(52) = 2.060(7); C(1)–B(1)–N(31) = 110.4(3), C(1)–B(1)–N(41) = 108.2(3), C(1)–B(1)–N(51) = 114.7(3), N(31)–B(1)–N(41) = 107.0(3), N(31)–B(1)–N(51) = 107.0(3), N(41)–B(1)–N(51) = 109.2(3), N(32)–Zn(1)–N(42) = 93.4(1), N(32)–Zn(1)–Cl(1) = 110.8(1), N(32)–Zn(1)–Cl(2) = 113.7(1), N(42)–Zn(1)–Cl(1) = 118.0(1), N(42)–Zn(1)–Cl(2) = 106.2(1), Cl(1)–Zn(1)–Cl(2) = 113.3(1); C(1)–B(1)–N(31)–N(32) = –61.1(4), C(1)–B(1)–N(41)–N(42) = 55.9(4), C(1)–B(1)–N(51)–N(52) = 178.1(3); N(31)N(32)C(33)C(34)C(35)//N(41)N(42)C(43)C(44)C(45) = 52.3.

The 3-*tert*-butylpyrazolyl derivative of **2**, $FlB(pz^{3\text{-}tBu})_3Li$ (**3**), crystallizes from THF/hexane in the monoclinic space group $P2_1c$ (**3**THF, Fig. 6). Contrary to the analogous phenyl substituted compound $PhB(pz^{3\text{-}tBu})_3Li$ [19], in which bonds between all three pyrazolyl rings and the lithium ion are established, the $[FlB(pz^{3\text{-}tBu})_3]^-$ moiety acts as a chelating bidentate ligand only. In this respect, the coordination mode observed for **3**THF in the solid state is similar to that of the parent compound **2**$(THF)_2$. A difference, however, lies in the coordination numbers of the lithium ions, which is four in the case of **2**$(THF)_2$ but only three in the case of **3**THF. As has already been observed for $PhB(pz^{3\text{-}tBu})_3Li$, the lower coordination number is associated with shorter lithium nitrogen bonds [i.e. **3**THF: Li(1)–N(32) = 1.929(7) Å, Li(1)–N(42) = 1.985(6) Å versus **2**$(THF)_2$: Li(1)–N(32) = 2.027(3) Å, Li(1)–N(42) = 2.040(4) Å], whereas the N–Li–N angle is virtually unaffected [i.e. **3**THF: N(32)–Li(1)–N(42) = 96.7(3)° versus **2**$(THF)_2$: N(32)–Li(1)–N(42) = 97.5(2)°].

Crystals of **4** (orthorhombic, $P2_12_12_1$; Fig. 7) were grown by layering a THF solution with toluene. X-ray crystallography reveals $ZnCl_2$ and an $Li(THF)_3^+$ fragment coordinated to the same fluorenylscorpionate entity. The $ZnCl_2$ unit is shown at the same position as occupied by $Li(THF)_2^+$ in **2**$(THF)_2$ while the $Li(THF)_3^+$ complex is attached to N(52) of the pyrazolyl ring which behaves as dangling substituent in **2**$(THF)_2$. Interestingly, LiCl is not eliminated under these conditions. This situation changed after a solution of **4** in CD_3CN had been kept in an NMR tube over a period of several days. Under these conditions, crystals of **5** (orthorhombic, *Pccn*; Fig. 8) formed. They consist of a Zn^{2+} ion coordinated by two $[FlBpz_3]^-$ ligands in a distorted tetrahedral fashion, which is reminiscent of the molecular structure of the anionic fragment $[FlBpz_3Lipz_3BFl]^-$ in **2**$_2(THF)_2(DMSO)_2$. Both molecules, $[FlBpz_3Lipz_3BFl]^-$ and **5**, are chiral but crystallize as racemic mixtures in the achiral orthorhombic space groups *Pbca* and *Pccn*, respectively. Their central metal ions Li^+ and Zn^{2+} are not located on the B···B

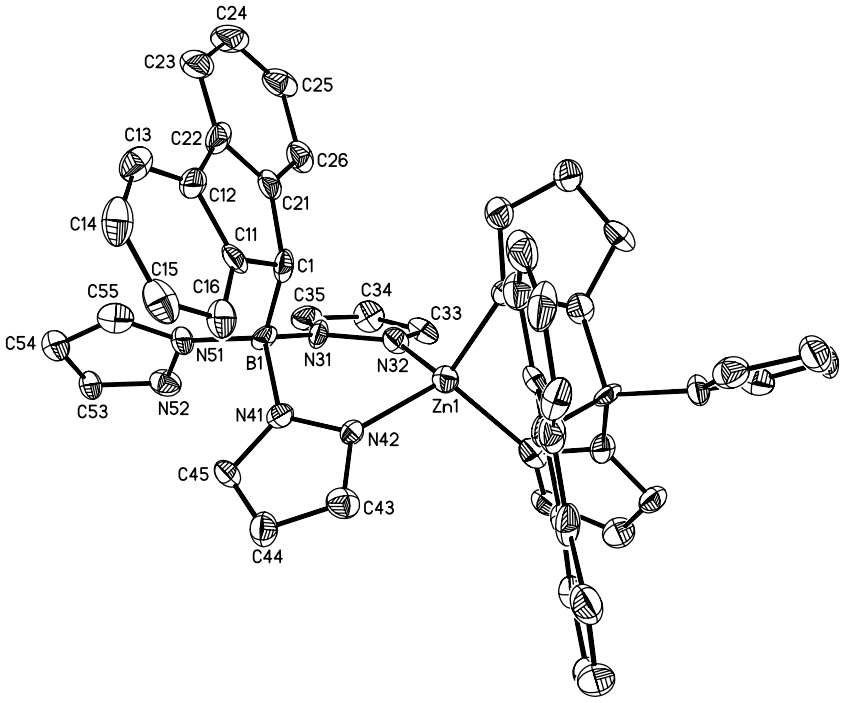

Fig. 8. Molecular structure and numbering scheme of compound **5**. Hydrogen atoms are omitted for clarity. Thermal ellipsoids are shown at the 50% probability level. Selected bond lengths (Å), angles (°), torsion angles (°), and dihedral angles (°): B(1)–C(1) = 1.604(12), B(1)–N(31) = 1.571(10), B(1)–N(41) = 1.565(11), B(1)–N(51) = 1.538(11), Zn(1)–N(32) = 1.995(7), Zn(1)–N(42) = 1.992(6); C(1)–B(1)–N(31) = 108.6(6), C(1)–B(1)–N(41) = 108.8(6), C(1)–B(1)–N(51) = 115.8(6), N(31)–B(1)–N(41) = 107.7(6), N(31)–B(1)–N(51) = 108.1(6), N(41)–B(1)–N(51) = 107.6(7), N(32)–Zn(1)–N(32$^{\#}$) = 119.5(4), N(32)–Zn(1)–N(42) = 97.7(3), N(32)–Zn(1)–N(42$^{\#}$) = 110.5(3), N(42)–Zn(1)–N(42$^{\#}$) = 122.5(4), N(42)–Zn(1)–N(32$^{\#}$) = 110.5(3); C(1)–B(1)–N(31)–N(32) = 61.8(9), C(1)–B(1)–N(41)–N(42) = −52.8(8), C(1)–B(1)–N(51)–N(52) = 164.5(7); N(31)N(32)C(33)C(34)C(35)// N(41)N(42)C(43)C(44)C(45) = 47.2. Symmetry transformation used to generate equivalent atoms: $-x + 3/2$, $-y + 1/2$, z (#).

axis but displaced by 0.494 Å ($[FlBpz_3Lipz_3BFl]^-$) and 0.812 Å (**5**).

3. Conclusion

Two fluorenyl/tris(pyrazol-1-yl)borate hybrid ligands have been developed: the parent system $FlBpz_3Li$ (**2**, Fl: 9-fluorenyl) and its 3-*tert*-butyl derivative $FlB(pz^{3\text{-}tBu})_3Li$ (**3**). Depending on the crystallization conditions and the solvents employed, different solid state structures of **2** were obtained. From THF/hexane, we have grown crystals consisting of monomeric units $Fl(pz)Bpz_2Li(THF)_2$, **2**$(THF)_2$, in which the lithium ion is coordinated by two chelating pyrazolyl rings and two THF molecules in a distorted tetrahedral geometry. Crystallization of **2** from THF/DMSO/toluene gave the centrosymmetric dimer $Fl(pz)Bpz_2Li(\mu_2\text{-}DMSO)_2Lipz_2B(pz)Fl$, (**2**DMSO)$_2$, featuring an Li_2O_2 core with two bridging DMSO ligands. A second crop of crystals was composed of ion pairs $[Li(THF)_2(DMSO)_2]^+[Li(\kappa^2N\text{-}FlBpz_3)_2]^-$, **2**$_2$(DMSO)$_2(THF)_2$. In contrast to **2**$(THF)_2$, the molecular structure of the sterically congested compound $FlB(pz^{3\text{-}tBu})_3Li$ (**3**) showed only one THF molecule coordinated to the lithium ion in the solid state (**3**THF). Addition of $ZnCl_2$ to a THF solution of **2** gives the dinuclear complex $(THF)_3Lipz(Fl)Bpz_2ZnCl_2$ (**4**), which, in acetonitrile, gradually transforms into the mononuclear species $Fl(pz)Bpz_2Znpz_2B(pz)Fl$ (**5**). In all these molecular structures, the $[FlBpz_3]^-$ ligands adopt very similar conformations with only two pyrazolyl rings bonded to the respective central metal, whereas the third pyrazolyl merely acts as dangling substituent. In future ligand design, this third donor site may therefore be replaced by a non-coordinating side chain (e.g. phenyl, *tert*-butyl) to exclude unwanted crosslinking reactions and to increase the solubility of our compounds in less polar solvents. Moreover, in all crystal structures investigated so far, the fluorenyl moiety adopts a position such that the C(9)–H(9) vector points toward the metal ion. Thus, the conformation required for fluorenide-metal binding after fluorenyl deprotonation is obviously readily accessible. Attempts to abstract the FlH-9 proton of **2** by LiH, *n*-BuLi, *tert*-BuLi, $LiN(SiMe_3)_2$ or $Zn[N(SiMe_3)_2]_2$ did not lead to satisfactory results. The use of potassium hydride, however, gives the corresponding deprotonated dianionic species **6** in quantitative yield. We are currently exploring the ligand properties of **6** towards selected transition metal ions in our laboratories.

4. Experimental

4.1. General considerations

All reactions and manipulations of air-sensitive compounds were carried out in dry, oxygen-free nitrogen using standard Schlenk ware. Solvents were freshly distilled under argon from Na-benzophenone (toluene, THF), Na/Pb alloy (hexane) or stored over 4 Å molecular sieves prior to use (C_6D_6, CD_3CN, DMSO). NMR: Bruker AMX 400, Bruker AMX 250, Bruker DPX 250 spectrometers. ^{11}B NMR spectra are reported relative to external $BF_3 \cdot Et_2O$. ^{7}Li NMR spectra are reported relative to external LiCl in D_2O. Unless stated otherwise, all NMR spectra were run at ambient temperature. Abbreviations: s = singlet; d = doublet; t = triplet; vtr = virtual triplet; dd = doublet of doublets; br = broad; n.r. = multiplet expected in the ^1H NMR spectrum but not resolved; n.o. = signal not observed; Me = methyl; Ph = phenyl; resonances marked with "*" belong to a magnetically unique pyrazolyl ring. Fluorenyllithium was prepared from fluorene and *n*-butyllithium in toluene. 3-*tert*-Butylpyrazole was synthesized according to the literature procedure [20,21]. Pyrazole and $BrB(NMe_2)_2$ were purchased from Aldrich.

4.2. Preparation of *1*

A slurry of fluorenyllithium (3.44 g, 20.00 mmol) in toluene (20 ml) was added dropwise with stirring at −78 °C to a solution of $BrB(NMe_2)_2$ (3.58 g, 20.02 mmol) in toluene (20 ml). After 1 h, the orange mixture was allowed to warm to ambient temperature, stirred overnight, filtered, and the orange coloured filtrate evaporated in vacuo to give a microcrystalline solid. Yield: 4.67 g (17.68 mmol, 88%). X-ray quality crystals of **1** were obtained by storing its hexane solution at −20 °C for several days.

^{11}B NMR (128.4 MHz, d_8-THF): 33.3 ($h_{1/2}$ = 190 Hz). ^1H NMR (250.1 MHz, d_8-THF): 1.93, 2.99 (2 × s, 2 × 6H, NCH_3), 4.14 (s, 1H, FlH-9), 7.25 (mult, 4H, FlH-2,3,6,7), 7.37 (d, 2H, $^3J_{HH}$ = 6.9 Hz, FlH-1,8), 7.82 (d, 2H, $^3J_{HH}$ = 6.5 Hz, FlH-4,5). ^{13}C NMR (62.9 MHz, C_6D_6): 39.5, 40.7 (NCH_3), 120.3 (FlC-4,5), 124.5 (FlC-1,8), 125.6, 126.9 (FlC-2,3,6,7), 141.7 (FlC-12,13), 149.1 (FlC-10,11), n.o. (C–B).

4.3. Preparation of *2*

Compound **1** (1.08 g, 4.09 mmol), lithium pyrazolide (0.30 g, 4.05 mmol) and pyrazole (0.56 g, 8.23 mmol) were dissolved in a mixture of toluene (20 ml) and THF (5 ml). The solution was heated to reflux for 8 h, whereupon a colourless precipitate formed which was isolated by filtration, washed with toluene (5 ml) and hexane (5 ml) and dried in vacuo. Yield: 1.35 g (3.51 mmol, 87%). X-ray quality crystals of **2**$(THF)_2$ were obtained by layering a THF solution of **2** with hexane. X-ray quality crystals of (**2**DMSO)$_2$ and **2**$_2(THF)_2$-$(DMSO)_2$ coprecipitated from a THF/DMSO solution of **2** which had been layered with toluene.

^{11}B NMR (128.4 MHz, CD_3CN): 1.9 ($h_{1/2}$ = 60 Hz). ^{11}B NMR (128.4 MHz, d_8-THF): 2.0 ($h_{1/2}$ = 80 Hz). ^1H NMR (250.1 MHz, CD_3CN): 4.95 (br, 1H, FlH-9), 5.47 (d, 2H, $^3J_{HH}$ = 7.3 Hz, FlH-1,8), 6.05 (br, 3H, pzH-4), 6.71 (br, 3H, pzH-3 or 5), 6.88 (vtr, 2H, $^3J_{HH}$ = 7.3 Hz, FlH-2,7), 7.22 (vtr, 2H, $^3J_{HH}$ = 7.5 Hz, FlH-3,6), 7.60 (br, 3H, pzH-5 or 3), 7.89 (d, 2H, $^3J_{HH}$ = 7.5 Hz, FlH-4,5). ^1H NMR (250.1 MHz, d_8-THF): 4.60 (s, 1H, FlH-9), 5.41 (d, 2H, $^3J_{HH}$ = 7.7 Hz, FlH-1,8), 6.11 (br, 3H, pzH-4), 6.82 (vtr, 2H, $^3J_{HH}$ = 7.5 Hz, FlH-2,7), 6.96 (br, 3H, pzH-3 or 5), 7.11 (vtr, 2H, $^3J_{HH}$ = 7.4 Hz, FlH-3,6), 7.62 (br, 3H, pzH-5 or 3), 7.77 (d, 2H, $^3J_{HH}$ = 7.5 Hz, FlH-4,5). ^{13}C NMR (62.9 MHz, CD_3CN): 49.7 (br, FlC-9), 104.4 (pzC-4), 120.4 (FlC-4,5), 125.3 (FlC-1,8), 125.9 (FlC-3,6), 127.1 (FlC-2,7), 135.5, 140.8 (pzC-3,5), 141.9 (FlC-12,13), 150.4 (FlC-10,11). ^{13}C NMR (62.9 MHz, d_8-THF): 103.9 (pzC-4), 119.8 (FlC-4,5), 125.1 (FlC-1,8), 125.2 (FlC-3,6), 126.7 (FlC-2,7), 129.7, 140.0 (pzC-5 or 3), 141.9 (FlC-12,13), 150.4 (FlC-10,11), n.o. (C–B). ^{7}Li NMR (155.5 MHz, CD_3CN): 0.46 ($h_{1/2}$ = 200 Hz). LR-MS (ESI, CD_3CN): m/z = 762 ($[C_{44}H_{36}B_2N_{12}Li]^-$, 100%), 377 ($[C_{22}H_{18}BN_6]^-$, 20%), 165 ($[C_{13}H_9]^-$, 11%). Anal. Calc. for $C_{44}H_{36}B_2Li_2N_{12}$ [768.33] × 2 C_2H_6OS [78.14] × 2 C_4H_8O [72.10]: C, 62.93; H, 6.04; N, 15.73. Found: C, 62.64; H, 5.91; N, 16.01%.

4.4. Preparation of *3*

n-Butyllithium in hexane (1.6 M, 2.5 ml, 4.00 mmol) was added with stirring at −78 °C to a solution of 3-*tert*-butylpyrazole (0.50 g, 4.00 mmol) in toluene (10 ml). After the reaction mixture had been warmed to room temperature, the colourless precipitate of lithium 3-*tert*-butylpyrazolide was collected on a frit and dried in vacuo. It was then dissolved in THF (2 ml) and treated with a solution of **1** (1.06 g, 4.00 mmol) and 3-*tert*-butylpyrazole (1.00 g, 8.00 mmol) in toluene (20 ml). The mixture was heated to reflux for 8 h, cooled to room temperature and evaporated to dryness under reduced pressure. The remaining yellow microcrystalline solid was washed with hexane (10 ml) and dried in vacuo. Yield of **3** × 1 THF: 1.53 g (2.45 mmol, 61%). X-ray quality crystals of **3**THF were obtained by layering a THF solution of **3** with hexane. Crystals of **3** × 1 DMSO were grown by layering a THF/DMSO solution of **3** with hexane.

^{11}B NMR (128.4 MHz, d_8-THF): 1.7 ($h_{1/2}$ = 120 Hz). ^1H NMR (400.1 MHz, d_8-THF, 0 °C): 1.39 (s, 27H,

CH_3), 4.70 (s, 1H, FlH-9), 5.21 (d, 2H, $^3J_{HH}$ = 7.4 Hz, FlH-1,8), 5.39, 5.81 (2 × br, 2 × 1H, pzH*-4,5), 6.06 (br, 2H, pzH-4), 6.76 (vtr, 2H, $^3J_{HH}$ = 7.5 Hz, FlH-2,7), 7.05 (vtr, 2H, $^3J_{HH}$ = 7.5 Hz, FlH-3,6), 7.08 (br, 2H, pzH-5), 7.71 (d, 2H, $^3J_{HH}$ = 7.4 Hz, FlH-4,5). ^{13}C NMR (100.6 MHz, d_8-THF): 31.2 (CH_3), 49.7 (br, *C* CH_3), 101.0 (br, pzC-4), 119.6 (FlC-4,5), 125.1 (FlC-3,6), 125.4 (FlC-1,8), 126.7 (FlC-2,7), 138.3 (br, pzC-3 or 5), 141.9 (FlC-12,13), 150.4 (FlC-10,11), 164.1 (br, pzC-5 or 3), n.o. (C–B). Anal. Calc. for $C_{34}H_{42}BLiN_6$ [552.50] × C_2H_6OS [78.14]: C, 68.56; H, 7.67; N, 13.33. Found: C, 68.80; H, 7.89; N, 13.04%. LR-MS (ESI^-): *m/z* = 545 ($[C_{34}H_{42}BN_6]^-$, 100%).

4.5. Preparation of **4** and **5**

To a solution of **2** × 2 THF (0.44 g, 0.83 mmol) in THF (15 ml) was added with stirring at room temperature a solution of $ZnCl_2$ (0.12 g, 0.84 mmol) in THF (5 ml). After stirring for 48 h, a small amount of colourless precipitate had been formed, which was removed by filtration. The clear filtrate was evaporated to dryness in vacuo. Yield of **4**: 0.60 g (0.81 mmol, 96%). X-ray quality crystals of **4** were grown by layering a THF solution with toluene. Crystals of **5** formed in an NMR tube from a solution of **4** in CD_3CN.

^{11}B NMR (128.4 MHz, CD_3CN): 1.8 ($h_{1/2}$ = 80 Hz). ^{1}H NMR (250.1 MHz, CD_3CN): 5.01 (br, 1H, FlH-9), 5.55 (d, 2H, $^3J_{HH}$ = 7.5 Hz, FlH-1,8), 6.37 (br, 3H, pzH-4), 6.77 (br, 3H, pzH-3 or 5), 6.97 (vtr, 2H, $^3J_{HH}$ = 7.5 Hz, FlH-2,7), 7.25 (vtr, 2H, $^3J_{HH}$ = 7.5 Hz, FlH-3,6), 7.88 (d, 2H, $^3J_{HH}$ = 7.5 Hz, FlH-4,5), 7.94 (br, 3H, pzH-5 or 3). ^{1}H NMR (250.1 MHz, CD_3CN, −20 °C): 4.93 (br, 1H, FlH-9), 5.41 (d, 2H, $^3J_{HH}$ = 7.7 Hz, FlH-1,8), 5.83 (vtr, 1H, $^3J_{HH}$ = 2.0 Hz, pzH*-4), 6.14 (d, 1H, $^3J_{HH}$ = 2.2 Hz, pzH*-3 or 5), 6.41 (vtr, 2H, $^3J_{HH}$ = 2.2 Hz, pzH-4), 6.77 (d, 2H, $^3J_{HH}$ = 2.0 Hz, pzH-3 or 5), 6.96 (vtr, 2H, $^3J_{HH}$ = 7.5 Hz, FlH-2,7), 7.25 (vtr, 2H, $^3J_{HH}$ = 7.5 Hz, FlH-3,6), 7.51 (d, 1H, $^3J_{HH}$ = 1.4 Hz, pzH*-5 or 3), 7.89 (d, 2H, $^3J_{HH}$ = 7.6 Hz, FlH-4,5), 8.01 (d, 2H, $^3J_{HH}$ = 1.6 Hz, pzH-5 or 3). ^{13}C NMR (62.9 MHz, CD_3CN): 105.7 (pzC-4), 120.7 (FlC-4,5), 125.1 (FlC-1,8), 126.2 (FlC-3,6), 127.3 (FlC-2,7), 137.6 (pzC-3 or 5), 142.0 (FlC-12,13, pzC-5 or 3), 149.5 (FlC-10,11), n.o. (C–B). ^{13}C NMR (62.9 MHz, CD_3CN, −20 °C): 105.4 (pzC*-4), 106.0 (pzC-4), 120.7 (FlC-4,5), 124.7 (FlC-1,8), 126.2 (FlC-3,6), 127.2 (FlC-2,7), 134.8 (pzC*-3 or 5), 137.6 (pzC-3 or 5), 141.6 (FlC-12,13), 141.8 (pzC*-5 or 3), 142.0 (pzC-5 or 3), 148.9 (FlC-10,11), n.o. (C–B). ^{7}Li NMR (155.5 MHz, CD_3CN): −2.63 ($h_{1/2}$ = 2 Hz). LR-MS (ESI^-, THF): 513 ($[C_{22}H_{18}BCl_2N_6Zn]^-$, 100%), 377 ($[C_{22}H_{18}BN_6]^-$, 14%), 203 ($[C_3H_3N_2Cl_2Zn]^-$, 13%). **4** Anal. Calc. for $C_{22}H_{18}BCl_2LiN_6Zn$ [520.47] × C_2H_6OS [78.14] × 2 C_4H_8O [72.10]: C, 51.74; H, 5.43; N, 11.31. Found: C, 51.86; H, 5.20; N, 11.66%. TXRF analysis: ratio Zn:Cl = 1:2.

4.6. Preparation of **6**

To a stirred solution of **2** × 2 THF (0.803 g, 1.520 mmol) in THF (20 ml) was added neat KH (0.080 g, 1.995 mmol) at ambient temperature. After 8 h, the orange solution was evaporated in vacuo to yield an orange coloured microcrystalline solid. Yield of **6** × 2 THF: 0.855 g (1.509 mmol, 99%).

^{11}B NMR (128.4 MHz, d_8-THF): 3.5 ($h_{1/2}$ = 450 Hz). ^{1}H NMR (250.1 MHz, d_8-THF): 5.78 (d, 2H, $^3J_{HH}$ = 8.2 Hz, FlH-1,8), 5.97 (vtr, 3H,$^3J_{HH}$ = 1.8 Hz, pzH-4), 6.35 (vtr, 2H, $^3J_{HH}$ = 7.1 Hz, FlH-3,6), 6.45 (vtr, 2H, $^3J_{HH}$ = 7.5 Hz, FlH-2,7), 6.91 (br, 3H, pzH-3 or 5), 7.39 (d, 3H, $^3J_{HH}$ = 1.9 Hz, pzH-5 or 3), 7.86 (d, 2H, $^3J_{HH}$ = 7.5 Hz, FlH-4,5). ^{13}C NMR (62.9 MHz, d_8-THF): 103.3 (pzC-4), 109.7 (FlC-3,6), 118.7 (FlC-1,8), 119.0 (FlC-4,5), 120.3 (FlC-2,7), 123.0 (FlC-12,13), 135.1, 139.9 (pzC-3,5), 140.8 (FlC-10,11), n.o. (C–B).

4.7. X-ray crystal structure determination of **1**, **2**(THF)$_2$, (**2**(DMSO)$_2$, **2**$_2$(THF)$_2$(DMSO)$_2$, **3**THF, **4**, and **5**

Data collection for all structures was performed on a STOE-IPDS-II diffractometer with graphite-monochromated Mo Kα-radiation. For (**2**DMSO)$_2$, **2**$_2$(THF)$_2$(DMSO)$_2$, **4** and **5** an absorption correction was performed with the MULABS [22] option in PLATON [23]. The structures were solved with direct methods [24] and refined against F^2 using full-matrix least-squares [25]. The contribution of the disordered solvent in (**2**DMSO)$_2$ was suppressed with the SQUEEZE [26] option in PLATON [23]. All non-H atoms have been refined anisotropically; the H atoms have been treated with a riding model, fixing their displacement parameter to 1.2 or 1.5 (for methyl groups) of the value of their parent atom. (**2**DMSO)$_2$: the molecule is located on a centre of inversion with half a molecule in the asymmetric unit. **3**THF: there are two molecules in the asymmetric unit. **4**: there are two molecules in the asymmetric unit; the absolute structure could be determined (Flack-*x*-parameter 0.008(8)). **5**: the molecule is located on a twofold rotation axis. As a result of that, there is just half a molecule in the asymmetric unit. **2**(THF)$_2$: the asymmetric unit contains half a tetrahydrofuran molecule which is disordered about a centre of inversion.

Acknowledgement

This work was generously supported by the Deutsche Forschungsgemeinschaft (DFG).

Appendix A. Supplementary data

Crystallographic data for the structure analyses have been deposited with the Cambridge Crystallographic Data Centre, CCDC Nos. 251802 (**1**), 251804 [**2**$(THF)_2$], 251798 [(**2**$DMSO)_2$], 251799 [$\mathbf{2}_2(THF)_2$-$(DMSO)_2$], 251801 [**3**THF], 251800 (**4**), and 251803 (**5**). Supplementary data associated with this article can be found, in the online version, at doi:10.1016/j.jorganchem.2004.11.004.

References

[1] N.J. Long, Metallocenes, Blackwell Science, London, 1998.
[2] A. Togni, R.L. Halterman (Eds.), Metallocenes, Wiley–VCH, New York, 1998.
[3] S. Trofimenko, Chem. Rev. 93 (1993) 943–980.
[4] S. Trofimenko, Scorpionates – The Coordination Chemistry of Polypyrazolylborate Ligands, Imperial College Press, London, 1999.
[5] F. Jäkle, K. Polborn, M. Wagner, Chem. Ber. 129 (1996) 603–606.
[6] F. Fabrizi de Biani, F. Jäkle, M. Spiegler, M. Wagner, P. Zanello, Inorg. Chem. 36 (1997) 2103–2111.
[7] E. Herdtweck, F. Peters, W. Scherer, M. Wagner, Polyhedron 17 (1998) 1149–1157.
[8] S.L. Guo, F. Peters, F. Fabrizi de Biani, J.W. Bats, E. Herdtweck, P. Zanello, M. Wagner, Inorg. Chem. 40 (2001) 4928–4936.
[9] S.L. Guo, J.W. Bats, M. Bolte, M. Wagner, J. Chem. Soc., Dalton Trans. (2001) 3572–3576.
[10] A. Haghiri, S.L. Guo, M. Bolte, M. Wagner, Dalton Trans. (2003) 2303–2307.
[11] I. Lopes, G.Y. Lin, A. Domingos, R. McDonald, N. Marques, J. Takats, J. Am. Chem. Soc. 121 (1999) 8110–8111.
[12] A. Otero, J. Fernández-Baeza, A. Antiñolo, J. Tejeda, A. Lara-Sánchez, L. Sánchez-Barba, A.M. Rodríguez, M.A. Maestro, J. Am. Chem. Soc. 126 (2004) 1330–1331.
[13] D. Roitershtein, Â. Domingos, N. Marques, Organometallics 23 (2004) 3483–3487.
[14] Part of this work was presented at the 227th ACS National Meeting, Anaheim, CA, USA. S. Bieller, F. Zhang, H.-W. Lerner, M. Wagner, Difunctional tris(pyrazol-1-yl)borates and scorpionate-cyclopentadienyl hybrid ligands; abstracts of papers INOR-054.
[15] H. Nöth, B. Wrackmeyer, in: P. Diehl, E. Fluck, R. Kosfeld (Eds.), NMR Basic Principles and Progress, vol. 14, Nuclear Magnetic Resonance Spectroscopy of Boron Compounds, Springer, Berlin, 1978.
[16] J. Mason, Multinuclear NMR, Plenum Press, New York, 1987.
[17] H.-O. Kalinowski, S. Berger, S. Braun, ^{13}C NMR-Spektroskopie, Thieme Verlag, Stuttgart, 1994.
[18] F.H. Allen, Acta Crystallogr., Sect. B 58 (2002) 380–388, Cambridge Crystallographic Database, Version 1.6 plus updates until July 2004.
[19] J.L. Kisko, T. Hascall, C. Kimblin, G. Parkin, J. Chem. Soc., Dalton Trans. (1999) 1929–1935.
[20] J. Elguero, E. Gonzalez, R. Jacquier, Bull. Soc. Chim. Fr. (1968) 707–713.
[21] S. Trofimenko, J.C. Calabrese, J.S. Thompson, Inorg. Chem. 26 (1987) 1507–1514.
[22] R.H. Blessing, Acta Crystallogr., Sect. A 51 (1995) 33–38.
[23] A.L. Spek, Acta Crystallogr., Sect. A 46 (1990) C34.
[24] G.M. Sheldrick, Acta Crystallogr., Sect. A 46 (1990) 467–473.
[25] G.M. Sheldrick, SHELXL-97: A Program for the Refinement of Crystal Structures, Universität Göttingen, Göttingen, Germany, 1997.
[26] P. van der Sluis, A.L. Spek, Acta Crystallogr., Sect. A 46 (1990) 194–201.